I&EC research
Industrial & Engineering Chemistry Research

Article

pubs.acs.org/IECR

Simultaneous Adsorption/Reduction of Bromate by Nanoscale Zerovalent Iron Supported on Modified Activated Carbon

Xiuqiong Wu,[†,‡] Qi Yang,*[,†,‡] Dechao Xu,[†,‡] Yu Zhong,[†,‡] Kun Luo,[†,‡,§] Xiaoming Li,*[,†,‡] Hongbo Chen,[†,‡] and Guangming Zeng[†,‡]

[†]College of Environmental Science and Engineering, Hunan University, Changsha, Hunan 410082, China

[‡]Key Laboratory of Environmental Biology and Pollution Control, Hunan University, Ministry of Education, Changsha, Hunan 410082, China

[§]Department of Bioengineering and Environmental Science, Changsha College, Changsha, Hunan 410003, China

S *Supporting Information*

ABSTRACT: Nanoscale zerovalent iron (nZVI) was reported as an effective material for the removal of bromate. However, its reactivity may be weakened due to its aggregation. In this study, nZVI was dispersed onto modified activated carbon (pretreated by nitric acid or/and ammonia) by impregnating carbon in ferrous sulfate with $NaBH_4$ as reducing agent. The nZVI supported on modified activated carbon (nZVI/MAC) was characterized by X-ray diffraction (XRD), scanning electron microscope (SEM), and transmission electron microscope (TEM). Good distribution of nZVI particles (about 50 nm) on the MAC was observed. The removal efficiencies of bromate by AC, nZVI, and nZVI/MAC were respectively evaluated. Experimental results indicated that nZVI/MAC showed the highest removal efficiency to bromate. In addition, the effects of initial bromate concentration (0.78−3.91 μmol/L) and pH (2.0−10.0) were investigated by batch experiments. Kinetic studies showed that the simultaneous adsorption and reduction of bromate by nZVI/MAC followed pseudo-first-order kinetics. Finally, bromine mass balance demonstrated that bromide was the only product for bromate reduction by nZVI/MAC, suggesting that bromate in aqueous solution was first adsorbed onto nZVI/MAC and subsequently reduced to innocuous bromide by nZVI.

1. INTRODUCTION

Bromate (BrO_3^-) is not commonly found in natural water, but it can be formed as one of the undesired disinfection byproducts (DBPs) after the ozonation or chlorination of water containing bromide (Br^-).[1,2] Several studies have confirmed that bromate is a potential human carcinogen for causing renal cell tumors in rats[3] and male mice.[4] The International Agency for Research on Cancer (IARC) has classified bromate as a group B-2 carcinogen.[5] The maximum contaminant level (MCL) for bromate in drinking water established by the World Health Organization (WHO) is only 10 μg/L (0.078 μmol/L)[2]. However, it has been found that the bromate concentration is as high as 150 μg/L following ozonation and advanced oxidation of drinking water.[6] Thus, nowadays, the control or removal of bromate in water has become a matter of special interest.

For the high solubility and stability, bromate is difficult to be removed once it is formed in water. Different approaches have been taken to decrease bromate concentrations in water. On the one hand, a number of research have focused on optimizing ozonation processes to minimize bromate formation. For example, pH suppression or ammonia addition during ozonation has been proven to be feasible to control bromate formation in some cases.[7] On the other hand, a variety of techniques to remove bromate after its formation have also been discussed, such as activated carbon adsorption,[8] zerovalent iron (Fe^0) reduction,[9] Pd/Al_2O_3 catalytic reduction,[10] and biological remediation.[11] Among them, chemical reduction provides a more efficient and cost-effective approach to reduce bromate. Nanoscale zerovalent iron (nZVI), for its larger specific surface area and higher reactivity, is widely applied in the various organic and inorganic contaminants reduction, such as chlorinated hydrocarbons,[12−14] azo dye,[15] nitrobenzene,[16] nitrate,[17] arsenic,[18,19] heavy metallic ions,[20−22] and so on. Recently, Wang et al successfully reduced 1 mg/L bromate using 0.1 g/L nZVI synthesized in aqueous ethanol.[23] Simultaneously, they found that the reduction process followed a second-order kinetic model with observed second-order rate constants (k_{obs}) of 25.7 to 219.0 min^{-1}, which was different than microsized ZVI in a pseudo-first-order kinetic model.[9]

However, similar to many other nanomaterials, nZVI particles exhibit a strong tendency to agglomerate into larger particles for its high surface energies and intrinsic magnetic interactions, resulting in the decrease of surface area and reactivity performance.[24] Immobilization of nZVI in supporting material such as silica,[25] organobentonite,[26] and multiwalled carbon nanotubes[22] is a promising approach to solve the problem above. Organobentonite supported nZVI particles was used to remove pentachlorophenol (PCP), and the kinetic results showed that the reaction rate for PCP removal could be enhanced 4.6-fold than the unsupported nZVI.[26] Compared with these supporting materials mentioned above, activated carbon (AC) has attracted intense interest due to its strong

Received: March 26, 2013
Revised: August 12, 2013
Accepted: August 13, 2013
Published: August 13, 2013

dx.doi.org/10.1021/ie4009524 | *Ind. Eng. Chem. Res.* 2013, 52, 12574−12581

sorption capacity, high surface area, porous structure, and relatively low cost.[27] AC granules with the size of 1.2−2.0 mm have been used to prevent nZVI aggregation.[28] The combination of AC and nZVI would take advantage of the two materials. The AC serves as an ideal support media for nZVI. Concertedly, the nZVI offers high reactive activity for bromated removal. Thus, it is interesting to evaluate the efficiency of bromate adsorption/reduction by nZVI supported on AC.

Carbon oxidation has been proven to be generally quite effective for iron loading.[18] Therefore, AC pretreated by nitric acid or/and ammonia was chosen as the supporting material to immobilize nZVI in this work. The nZVI supported on modified activated carbon (nZVI/MAC) was characterized by scanning electron microscopy (SEM), transmission electron microscopy (TEM), and X-ray diffraction (XRD). The efficiency and kinetic analysis of bromate removal by nZVI/MAC were investigated. In addition, the effects of initial bromate concentration and pH values were evaluated. Finally, the possible mechanism involved in the process of bromate removal by nZVI/MAC was also elucidated.

2. EXPERIMENTAL SECTION

2.1. Materials and Chemicals. A commercial coconut shell-based activated carbon (particles sieved: 0.55−0.27 mm) was purchased from Xinsen Carbon Industry, China. Ferrous sulfate heptahydrate (≥99%), sodium borohydride (≥98.0%), polyethylene glycol-4000 (PEG-4000), and absolute alcohol (≥99.7%) were used for the synthesis of nZVI. Sodium bromate (≥99.7%) was used in the preparation of bromate stock solution. All chemicals used in the experiments were of analytical grade and used as received without any further purification. All solutions were prepared with Milli-Q ultrapure water (18.2 MΩcm).

2.2. Synthesis of nZVI/MAC. The AC was first subjected to boiling water for 30 min to remove partial impurities, and it was named AC_{H2O}. Then, AC_{H2O} was washed respectively by 30% HNO_3 for 2 h at 80 °C and 25% $NH_3·H_2O$ for 4 h at 60 °C, designated respectively as AC_{HNO3} and AC_{NH3}. Finally, AC_{HNO3} treated sequentially by 25% $NH_3·H_2O$ for 4 h was labeled as AC_{HN}. The MAC was thoroughly washed with distilled water until the pH of the solution stabilized, and then it was dried at 105 °C for 24 h. The surface chemical properties of MAC were determined by Boehm titration[29] and mass titration[30] methods.

Nanoscale zerovalent iron particles were synthesized by a traditional liquid phase reduction method. 2.00 g of $FeSO_4·7H_2O$ was dissolved in 100 mL of solution (30 mL ultrapure water and 70 mL absolute ethanol), and then 0.5 g of PEG-4000 was added as a dispersant to reduce nZVI aggregation in the ferrous sulfate solution. After the dropwise addition of 45 mL of 1 mol/L $NaBH_4$, the mixture was stirred continuously for 30 min. The reaction could be represented as eq 1:

$$Fe^{2+} + 2BH_4^- + 6H_2O = Fe^0 + 2B(OH)_3 + 7H_2 \qquad (1)$$

The metal particles formed were settled and separated from the liquid phase by vacuum filtration using filter papers. Then the solids were washed with water and ethanol for several times and finally freeze-dried. To prevent synthesized nZVI from passivation by oxygen, the preparation process was operated under a nitrogen atmosphere. nZVI supported on MAC was prepared by a similar procedure as described above, except for that 4.0 g of different MAC (AC_{H2O}, AC_{HNO3}, AC_{NH3}, and AC_{HN}) was soaking in 100 mL of $FeSO_4·7H_2O$ solution with PEG-4000 as the dispersant. Before the addition of the $NaBH_4$ solution, the suspension was mixed in an ultrasonic bath for 2 h, and then further stirred for 1 h with nitrogen purging. The final products were labeled as nZVI/(AC_{H2O}, AC_{HNO3}, AC_{NH3}, AC_{HN}), respectively.

2.3. Characterization. The crystal structure of nanoparticles immobilized AC was examined with an X-ray diffraction (XRD, Siemens D5000, Germany) analysis with Cu Kα radiation (λ = 1.5406 Å) operating at 50 kV voltage and 30 mA current.

The morphology of nZVI and nZVI/MAC was observed by transmission electron microscope (TEM, JEM-2100, Japan) and scanning electron microscopy (SEM, JSM-6700F, Japan).

2.4. Batch Experiments for Bromate Adsorption/Reduction. Batch experiments were conducted in a 300 mL sealed headspace glass Erlenmeyer flask to investigate the adsorption and (or) reduction ability of samples to bromate. A certain amount of AC_{HN}, commercial iron powder, or nZVI was added followed by the addition of 300 mL of bromate solution at 1.56 μmol/L. The amount of AC_{HN}, commercial iron powder, and nZVI in the solution was 50, 10, and 10 mg/L respectively. Similarly, a certain amount of nZVI/MAC was added, in which the content of Fe was 5 mg/L. The initial pH of the solution was 6.8 without the addition of buffers. Each flask was shaken laterally in a water bath shaker with a rate of 150 rpm at room temperature. At given time intervals, a small amount of sample was withdrawn and filtered through a 0.22 μm glass microfiber filter. The filtered solution was taken for the analysis of bromate and bromide.

Some factors affecting the bromate removal of nZVI/MAC were investigated. Experiments were carried out with the procedure and under the same conditions as described above. Initial solution pH values between 2.0 and 10.0 adjusted by 0.1 M H_2SO_4 or 0.1 M NaOH were studied. The effect of initial bromate concentration was considered at concentrations of 0.78, 1.56, 2.34, 3.13, and 3.91 μmol/L.

2.5. Analytical Method. Quantitative analysis of bromate and bromide was performed in an ion chromatograph (ICS-900, Dionex) with a low-conductivity mobile phase. Sodium carbonate and sodium bicarbonate buffer solution was used as the effluent at a flow rate of 1.0 mL/min. The solution pH was monitored with a pH meter (FE20, Mettler Tolima Instrument).

3. RESULTS AND DISCUSSION

3.1. Characterization of nZVI/MAC. *3.1.1. XRD.* Figure 1 shows the representative XRD patterns of the nZVI/AC_{H2O}, nZVI/AC_{NH3}, nZVI/AC_{HNO3}, nZVI/AC_{HN}, and nZVI. In the pattern of supported nanoparticles and AC in Figure 1 (a−e), a relatively broader shoulder peak (C) corresponding to amorphous carbon at the 2θ of 22°−24° can be observed.[16] The gradually weakened diffraction peak suggested that the internal pore of AC collapsed partially since the acid or/and alkali pretreatment led to the disorderly morphology and lower crystallization.[31]

The apparent peak appeared at 2θ of 43°−45° in all samples except for AC (Figure 1a), suggesting the presence of α-Fe^0 in both nZVI/MAC and unsupported nZVI. However, the peak at 43°−45° of nZVI/MAC was weaker and broader than that of nonsupported nZVI, which indicated that nZVI supported on MAC was smaller than unsupported nZVI. Compared to

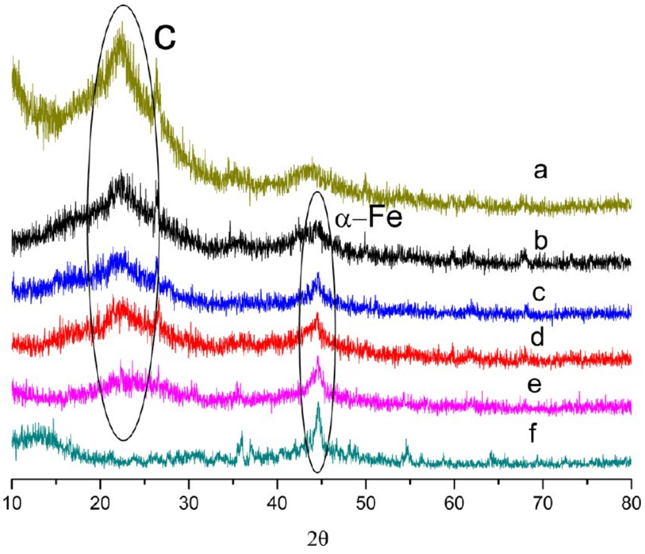

Figure 1. XRD images of the nZVI/MAC (a) AC; (b) nZVI/AC_{H2O}; (c) nZVI/AC_{NH3}; (d) nZVI/AC_{HNO3}; (e) nZVI/AC_{HN}; and (f) nZVI.

nonsupported nZVI, the large specific surface area may promote the immobilization of iron nanoparticles on MAC with higher surface reactivity. In addition, a small peak in Figure 1 (b−f) at 2θ of 35°−40° elucidated that nZVI immobilized on MAC and unsupported nZVI were partially oxidized to Fe_2O_3 or Fe_3O_4.[32] Because of the small size of the particles and low content of these samples (less than 10%), the peaks in the XRD pattern were relatively broad.[14,23,33] It was difficult to determine the crystalline structure and the main particle size of the nZVI via XRD, hence a detailed analysis of the samples was carried out by SEM.

3.1.2. SEM and TEM. SEM was used to obtain the surface morphology and the structure of the nZVI immobilized on MAC. The 300× magnification SEM image clearly shows nanoparticles (white dots) throughout the surface of AC (see Figure 2 (a-d)), indicating the successful immobilization of ZVI nanoparticles. It was noteworthy that the distribution of ZVI nanoparticles among AC displayed some differences. The bulk agglomeration of nZVI was observed in AC_{H2O}, AC_{NH3}, and AC_{HNO3}, while a relatively even distribution of ZVI nanoparticles was observed in the AC_{HN}. It has been proven that the interaction between AC and metal particles was influenced by point of zero charge (PZC)[34] and surface functional groups of AC.[35] Functional groups concentrations determined via the Boehm titration method are shown in Table S1. It can be found that the surface chemical structures of plain and modified AC were highly diverse. The acidic groups of AC_{HNO3} were seven times higher than that of AC_{H2O}. Simultaneously, acid treatment of AC induced a significant decrease of pH_{pzc}. However, the opposite evolution was observed after ammonia-treatment. Adsorption of iron ions on the MAC was strengthened by electrostatic interactions between the negatively charged AC surface and the positively charged iron ions in solution. Moreover, acidic oxygen groups can behave as ion-exchange centers, retaining iron ion and releasing protons to aqueous solution, which contributed to the adsorption of iron ion on AC.[18,36] AC_{HN} possesses less acidic functional groups and relatively lower pH_{pzc} (Table S1); therefore, it might load more iron ions compared to AC_{NH3} and AC_{H2O} but less than AC_{HNO3}.

Figure S1 illustrates size distribution histogram of nanoparticle immobilized on different MAC. The average particle sizes of ZVI nanoparticles, determined by SEM images, were 45.88, 45.51, 53.6, and 48.32 nm on AC_{H2O}, AC_{NH3}, AC_{HNO3}, and AC_{HN}, respectively. The larger particle size of ZVI nanoparticles on AC_{HNO3} may be attributed to the oxidation of AC by nitric acid which produced highly acidic oxygen-containing groups and displayed lowest pH_{pzc}. The AC_{HNO3} adsorbed excessive Fe^{2+} that was subsequently reduced to nZVI by KBH_4, and nZVI aggregated in bulk on AC surface, resulting in large nanoparticle size. In addition, the TEM images of nZVI/AC_{HN} (Figure S3a, Supporting Information) showed that there were roughly spherical nZVI particles (∼36−100 nm in diameter) in the pores of AC. However, the nonsupported nZVI aggregated severely, leading to chainlike iron nanoparticles with large size (Figure S3b). The observed results suggested that the developed porous structure and huge specific surface area of AC could minimize the agglomeration of nZVI and thus maintain high dispersion and reactivity of nZVI, which may allow good accessibility of contaminants to the surface of nanoparticles and sequential reduction.

3.2. Adsorption/Reduction of Bromate by nZVI/MAC.

3.2.1. Effect of Supported nZVI on Bromate Removal. Figure 3 presents the results of adsorption and/or reduction of the bromate onto/by ZVI, AC, nZVI, and nZVI/MAC. It was found that the commercial Fe^0 powder hardly showed the reductive ability to bromate during the whole process, while a higher efficiency (77.25%) by nZVI was achieved within 5 min. The increased efficiency was obviously related to the difference of particle size between commercial iron and nZVI (nZVI about 100 nm, Fe^0 powders approximate 150 μm). The smaller particles size means larger specific surface area which offers more interfaces for ZVI and bromate.[37] In comparison, the nZVI/AC_{HN} composite showed a higher efficiency of bromate removal. The removal efficiency of bromate by nZVI/AC_{HN} reached 95.66% after 5 min. It was not only much higher than that by nZVI (77.25%) but also distinctly superior to the simple summation (83.12%) of reduction by nZVI and adsorption (5.87%) by AC_{HN}. The results indicated that the bromate removal by nZVI/AC_{HN} was not a simple summation of adsorption and reduction. There must be synergetic adsorption and reduction for bromate removal.

Close contact between bromate and iron surface is required since the bromate reduction by nZVI is surface mediated. The adsorption capacity of AC_{HN} facilitated the mass transfer of bromate in the solution onto AC_{HN}, which promoted the contact of bromate with nZVI by increasing the local concentration of bromate in the vicinity of iron nanoparticles, enhancing bromate removal. In conclusion, nZVI played the dominant role in the reduction of bromate using nZVI/MAC, while MAC acted as a dispersant of nZVI and partially absorbed bromate. Similar synergetic effect had also been reported on the PCP removal by nZVI immobilized on organobentonite[26] and chromium(VI) removal by nZVI supported on multiwalled carbon nanotubes.[22] In comparison, the removal efficiencies of bromate by nZVI/AC_{H2O}, nZVI/AC_{NH3}, and nZVI/AC_{HNO3} within 5 min were only 54.12%, 81.76%, and 92.14%, much lower than that by nZVI/AC_{HN}, which might be due to the relatively uniform distribution of ZVI nanoparticles in AC_{HN} (Figure 2).

3.2.2. Kinetic Study on Adsorption/Reduction of Bromate. In order to investigate the mechanism of reduction and potential rate-limiting steps such as mass transport and

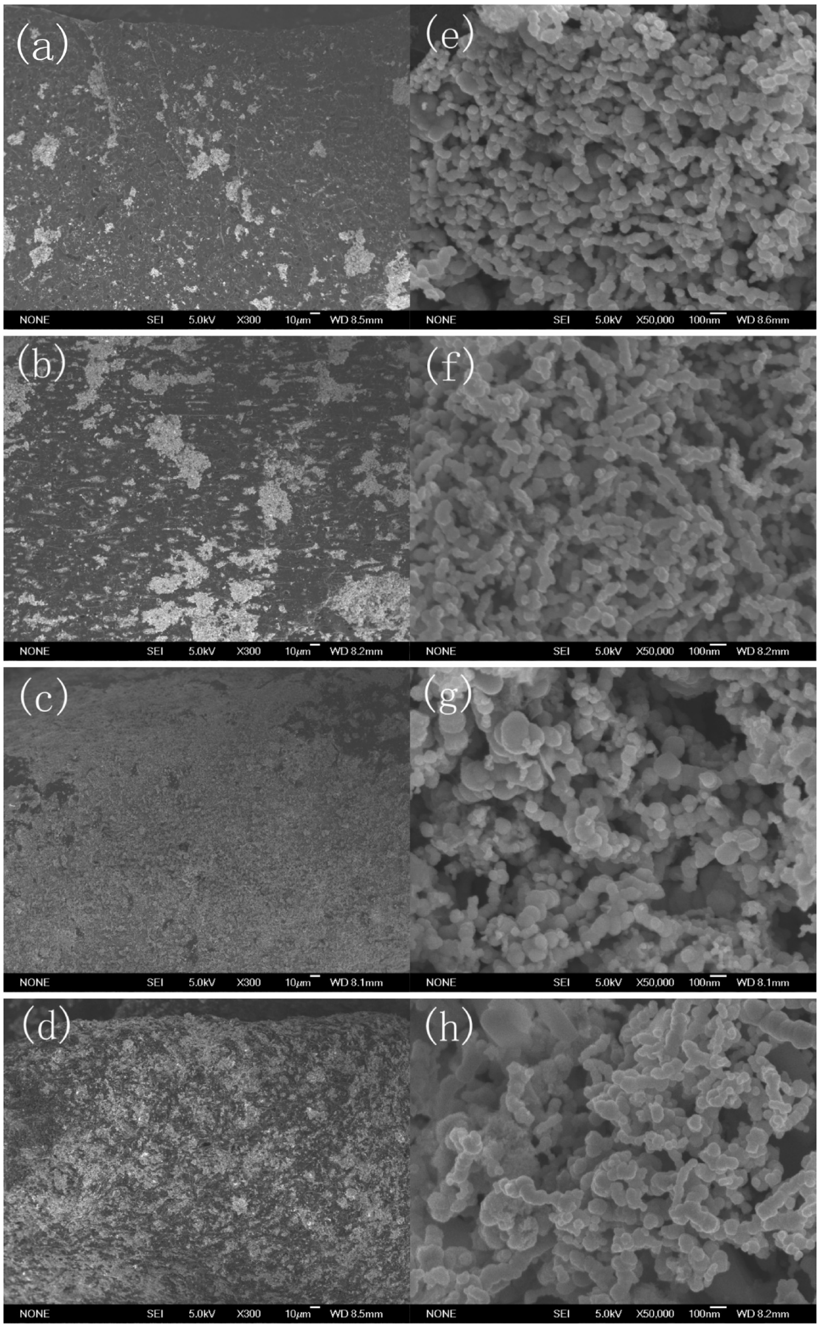

Figure 2. SEM (×300 magnification) images of (a) nZVI/AC_{H2O}, (b) nZVI/AC_{NH3}, (c) nZVI/AC_{HNO3}, and (d) nZVI/AC_{HN}. SEM (×50,000 magnification) images of (e) nZVI/AC_{H2O}, (f) nZVI/AC_{NH3}, (g) nZVI/AC_{HNO3}, and (h) nZVI/AC_{HN}.

chemical reduction reaction processes, kinetic models were used to test the experimental data.

A pseudo-first-order kinetic model has been successfully used to investigate the reduction of contaminant by supported nZVI.[28,38] Figure 3 shows linearized plots ($\ln(C_0/C)$ vs time) of the experimental and model-simulated kinetic data. Table 1 gives the fitted model parameters. The kinetics of bromate removal conformed to the pseudo-first-order model eq 2. The R^2 higher than 0.95 except for nZVI/AC_{H2O}, which indicated fairly good model fitting, was obtained

$$\ln \frac{C}{C_0} = k_{obs}t \tag{2}$$

where C_0 (μmol/L) is the initial concentration of bromate, C (μmol/L) is the concentration of bromate at time t (min), and k_{obs} (min^{-1}) is the observed rate constant of pseudo-first-order reaction.

Table 1 shows the k_{obs} for nZVI/MAC except for nZVI/AC_{H2O} were all greater than that of unsupported nZVI. In addition, the k_{obs} of bromate by nZVI/AC_{HN} was 4.15 times higher than that by nZVI alone, which should be contributed that the immobilized nZVI maybe react with higher concentration of bromate in the local region due to the adsorption of AC and nZVI, thus enhancing bromate reduction in nZVI/MAC. Tseng et al.[28] synthesized granular activated carbon/zerovalent iron composites for simultaneous adsorption/dechlorination of trichloroethylene (TCE) and concluded

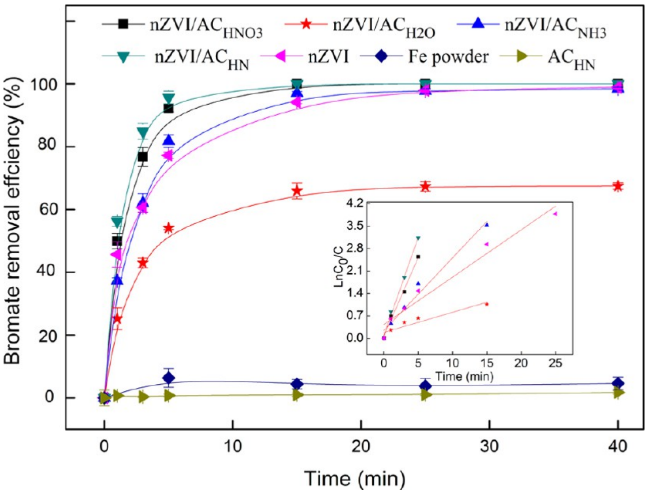

Figure 3. Comparison of bromate removal by AC, nZVI, Fe^0 powder, and various nZVI/MAC. Insert: modeling of the kinetics by fitting to the pseudo-first-order reaction. Reaction condition: initial bromate concentration 1.56 μmol/L; pH 6.8; T 25 °C.

Table 1. Parameters for Kinetics of Bromate Removal by nZVI or nZVI/MAC

samples	k_{obs} (min^{-1})	R^2
nZVI/AC$_{H2O}$	0.0623	0.8537
nZVI/AC$_{NH3}$	0.2265	0.9763
nZVI/AC$_{HNO3}$	0.4897	0.9916
nZVI/AC$_{HN}$	0.6113	0.9956
nZVI	0.1474	0.9608

that the synthesized material exhibited a higher potential for TCE removal than the individual use of either GAC or ZVI.

3.2.3. Effect of Initial Bromate Concentration. The influence of initial bromate concentrations on removal efficiency by nZVI/AC$_{HN}$ was investigated in the range from 0.78 to 3.91 μmol/L. Figure 4 shows the k_{obs} and initial rate for bromate removal as a function of initial bromate concentration. The final removal efficiencies of bromate kept near 100% within the range of initial bromate concentrations investigated. The k_{obs} for bromate removal declined from 0.7778 min^{-1} at 0.78 μmol/L to 0.2973 min^{-1} at 3.91 μmol/L. Although the k_{obs} decreased with increasing of the initial bromate concentration, the initial rate constant for bromate removal increased from 0.607 μmol L^{-1} min^{-1} at 0.78 μmol/L to 1.139 μmol L^{-1} min^{-1} at 3.13 μmol/L and then kept nearly constant with the increasing of initial bromate concentration (Figure 4b). The above observed trends were coincident to the Langmuir–Hinshelwood model (eq 3). Then the L–H model was used, and a good fit was achieved between the initial bromate concentration (C_0) and the initial rate constant (r_0) with the reaction rate constant (k_1) and adsorption coefficient (b) of 1.612 μmol L^{-1} min^{-1} and 0.7937 L μmol^{-1}, respectively.

$$\frac{1}{r_0} = \frac{1}{bk_1}\cdot\frac{1}{C_0}\frac{1}{k_1} \tag{3}$$

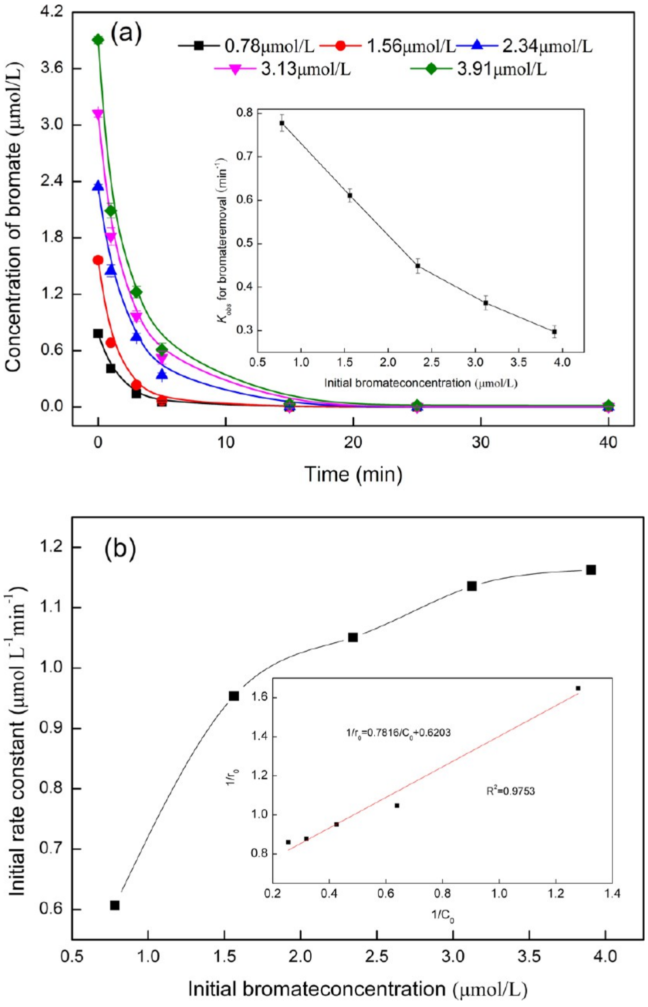

Figure 4. (a) Relationship of bromate concentration versus time for initial concentrations of 0.78, 1.56, 2.34, 3.13, and 3.91 μmol/L bromate removal by nZVI/AC$_{HN}$. The inset is plots of the variation k_{obs} with initial bromate concentration. (b) Initial rate constant as a function of initial bromate concentration. The inset shows linear plot of $1/r_0$ versus $1/C_0$.

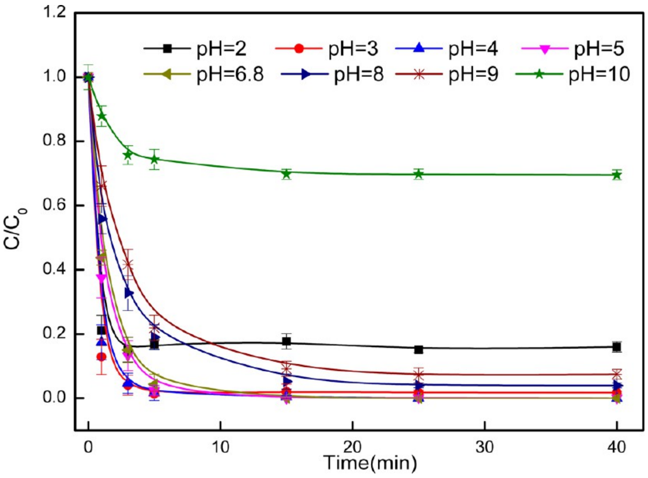

Figure 5. Effect of initial pH on bromate reduction by nZVI/AC$_{HN}$.

The plot of $1/r_0$ versus $1/C_0$ is given in Figure 4b. It was obvious that the correlation coefficient was close to 1, which indicated that the reaction rate was positively related to the amount of bromate in nZVI/MAC. These results all suggested that bromate in solution was first adsorbed onto a limited number of reactive sites on the surface of supported nanoparticles and subsequently undergo the reduction reaction at these sites by the pseudo-first-order kinetics. Similar results have also been reported on dechlorination of chlorinated

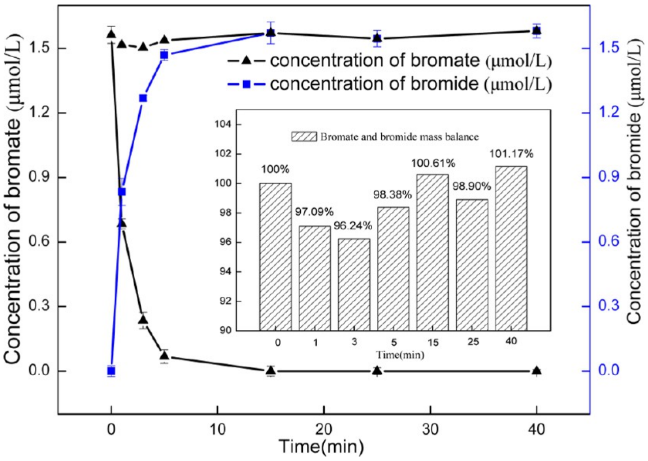

Figure 6. Bromine species in bromate reduction by nZVI/AC_{HN} (Insert represents bromine mass balance.).

hydrocarbons by bimetallic Ni/Fe immobilized on polyethylene glycol-grafted microfiltration membranes[39] and PCP removal by nZVI immobilized on organobentonite.[26]

3.2.4. Effect of Initial pH. The effect of initial pH on the reduction of bromate from solution by nZVI/AC_{HN} is shown in Figure 5. The solution pH value was adjusted respectively to 2.0, 3.0, 4.0, 5.0, 6.8, 8.0, 9.0, and 10.0 with either 0.1 M H_2SO_4 or NaOH. The removal efficiency of bromate was 30.46−100% in the pH range of 2−10, but the efficiency was only slightly affected when the pH value was between 3 and 8, which was the favorable pH. Except for pH 2.0 and 10.0, the reduction of bromate could fit the pseudo-first-order model quite well. k_{obs} was respectively 0.7875, 0.7187, and 0.3168 min^{-1}, when the initial pH value was 3.0, 5.0, and 8.0, indicating that the reduction rate increased as pH decreased, which has also been reported in other studies.[21,40] Two reasons should cause the acceleration of bromate removal by nZVI at the low pHs. First, the iron oxide layers covering the nZVI dissolved more under acidic conditions, which made nZVI more exposed and contributed to more rapid reduction reaction between bromate and nZVI. Second, low pHs led the surface of the nZVI to be protonated to a higher extent, which improved the strong attraction between the negatively charged bromate and the positively charged surface. A similar pH-dependence trend in As(III) and bromate removal by nZVI has also been observed.[19,23] But under extremely acidic conditions (pH = 2.0), the nZVI dissolved quickly into the solution, resulting in an insufficient amount of nZVI for the release of ferrous ions and electrons, which was in accordance with that reported by Shu et al.[15] Nevertheless, surface passivated layers were formed at high pH values due to precipitation of metal hydroxide and metal carbonates, which blanketed the nZVI's shell and reduced the removal efficiency of bromate at high pH values.

3.3. Mechanism of Bromate Removal by nZVI/MAC.

Figure 6 shows the concentrations of two bromine species, i.e., bromate and bromide, and the total bromine mass of the two species during bromate reduction process by nZVI/AC_{HN}. The results illustrated that bromide was the only product for bromate reduction, and the bromine mass balance was in the range of 96.24−101.17% during the experimental course, indicating that the removal of bromate by nZVI/AC_{HN} was dominantly due to the reduction of nZVI instead of the adsorption by AC_{HN}. Tseng et al.[28] concluded that imbedded and dispersed ZVI particles were present in close proximity to sorbed TCE on the GAC and thus might increase the reductive reactivity of ZVI during the course of dynamic sorption/desorption processes. The TEM results also demonstrated that nZVI particles were completely dispersed on the surface of MAC.

On the basis of the results described above, Figure 7 showed the possible two-step mechanism for the removal of bromate by nZVI/MAC. First, bromate in solution was absorbed quickly on the surface of nZVI/MAC since nZVI and MAC could absorb the ion.[41,42] Then, the adsorbed bromate was reduced by nZVI and the reduced products, bromide, entered into the solution.

4. CONCLUSIONS

In summary, MAC has been applied as the support for nZVI in order to prevent effectively the agglomeration of nanoparticles. Results of batch experiments with bromate as the objective pollutant demonstrated that nZVI/AC_{HN} could effectively remove bromate from water, possessing higher removal efficiency than both AC_{HN} and unsupported nZVI. Bromate was adsorbed and then reduced sequentially to bromide by nZVI/AC_{HN}. The k_{obs} of bromate by nZVI/AC_{HN} was 4.15 times higher than that by unsupported nZVI. The initial rate for bromate removal by nZVI/AC_{HN} increased with the increase of initial bromate concentration. In addition, the bromate reduction was pH-dependent and the k_{obs} increased as pH decreased, except for under extremely acidic conditions. In view of this, the nZVI/AC_{HN} could be suggested as a potential

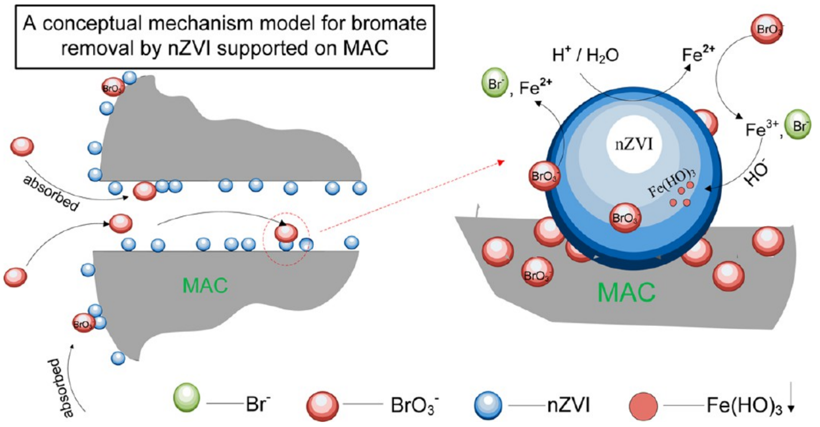

Figure 7. A schematic diagram of removal mechanism of bromate by nZVI/MAC.

material to remove organic and inorganic contaminants due to its synergistic effects of adsorption capacity and significant reduction reactivity.

■ ASSOCIATED CONTENT

Ⓢ Supporting Information

Table S1, Boehm's titration and mass titration result of different activated carbons; Figure S1, histogram of particle sizes of nZVI nanoparticles determined by SEM images: (a) nZVI/AC$_{H2O}$, (b) nZVI/AC$_{NH3}$, (c) nZVI/AC$_{HNO3}$, and (d) nZVI/AC$_{HN}$; Figure S2, SEM image of AC; Figure S3, TEM image of nZVI/AC$_{HN}$ and unsupported nZVI. This material is available free of charge via the Internet at http://pubs.acs.org.

■ AUTHOR INFORMATION

Corresponding Authors

*Phone: +86-731-88822829. Fax: +86-731-88822829. E-mail: yangqi@hnu.edu.cn (Q.Y.).
*Phone: +86-731-88822829. Fax: +86-731-88822829. E-mail: xmli@hnu.edu.cn (X.-M.L.).

Notes

The authors declare no competing financial interest.

■ ACKNOWLEDGMENTS

This research was financially supported by the project of National Natural Science Foundation of China (No. 51078128), International Science & Technology Cooperation Program of China (Nos. 2011DFA90740 and 2012DFB30030-03).

■ REFERENCES

(1) Gunten, U. V. Ozonation of Drinking Water: Part II. Disinfection and By-Product Formation in Presence of Bromide, Iodide or Chlorine. *Water Res.* **2003**, *37*, 1469.

(2) Weinberg, H. S.; Delcomyn, C. A.; Unnam, V. Bromate in Chlorinated Drinking Waters: Occurrence and Implications for Future Regulation. *Environ. Sci. Technol.* **2003**, *37*, 3104.

(3) Kurokawa, Y.; Takayama, S.; Konishi, Y.; Hiasa, Y.; Asahina, S.; Takahashi, M.; Maekawa, A.; Hayashi, Y. Long-Term in Vivo Carcinogenicity Tests of Potassium Bromate, Sodium Hypochlorite, and Sodium Chlorite Conducted in Japan. *Environ. Health Perspect.* **1986**, *69*, 221.

(4) DeAngelo, A. B.; George, M. H.; Kilburn, S. R.; Moore, T. M.; Wolf, D. C. Carcinogenicity of Potassium Bromate Administered in the Drinking Water to Male B6C3F1Mice and F344/N Rats. *Toxicol Pathol.* **1998**, *26*, 587.

(5) Moore, M. M.; Chen, T. Mutagenicity of Bromate: Implications for Cancer Risk Assessment. *Toxicology* **2006**, *221*, 190.

(6) Krasner, S. W.; Glaze, W. H.; Weinberg, H. S.; Daniel, P. A.; Najm, I. N. Formation and Control of Bromate During Ozonation of Waters Containing Bromide. *J. - Am. Water Works Assoc.* **1993**, *85*, 73.

(7) Williams, M. D.; Coffey, B. M.; Krasner, S. W. Evaluation of pH and Ammonia for Controlling Bromate during Cryptosporidium Disinfection. *J. - Am. Water Works Assoc.* **2003**, *95*, 82.

(8) Wang, L.; Zhang, J.; Liu, J.; He, H.; Yang, M.; Yu, J.; Ma, Z.; Jiang, F. Removal of Bromate Ion Using Powdered Activated Carbon. *J. Environ. Sci.* **2010**, *22*, 1846.

(9) Li, X.; Chii, S. The Effects of Operational Parameters and Common Anions on the Reactivity of Zero-Valent Iron in Bromate Reduction. *Chemosphere* **2007**, *66*, 1652.

(10) Chen, H.; Xu, Z.; Wan, H.; Zheng, J.; Yin, D.; Zheng, S. Aqueous Bromate Reduction by Catalytic Hydrogenation over Pd/Al_2O_3 Catalysts. *Appl. Catal. B: Environ.* **2010**, *96*, 307.

(11) Assunção, A.; Martins, M.; Silva, G.; Lucas, H.; Coelho, M. R.; Costa, M. C. Bromate Removal by Anaerobic Bacterial Community: Mechanism and Phylogenetic Characterization. *J. Hazard. Mater.* **2011**, *197*, 237.

(12) Zhan, J.; Kolesnichenko, I.; Sunkara, B.; He, J.; McPherson, G. L.; Piringer, G.; John, V. T. Multifunctional Iron-Carbon Nanocomposites through an Aerosol-Based Process for the in Situ Remediation of Chlorinated Hydrocarbons. *Environ. Sci. Technol.* **2011**, *45*, 1949.

(13) Choi, H.; Al-Abed, S. R.; Agarwal, S.; Dionysiou, D. D. Synthesis of Reactive Nano-Fe/Pd Bimetallic System-Impregnated Activated Carbon for the Simultaneous Adsorption and Dechlorination of PCBs. *Chem. Mater.* **2008**, *20*, 3649.

(14) Chang, C.; Lian, F.; Zhu, L. Simultaneous Adsorption and Degradation of γ-HCH by nZVI/Cu Bimetallic Nanoparticles with Activated Carbon Support. *Environ. Pollut.* **2011**, *159*, 2507.

(15) Shu, H. Y.; Chang, M. C.; Chen, C. C.; Chen, P. E. Using Resin Supported Nano Zero-Valent Iron Particles for Decoloration of Acid Blue 113 Azo Dye Solution. *J. Hazard. Mater.* **2010**, *184*, 499.

(16) Ling, X.; Li, J.; Zhu, W.; Zhu, Y.; Sun, X.; Shen, J.; Han, W.; Wang, L. Synthesis of Nanoscale Zero-Valent Iron/Ordered Mesoporous Carbon for Adsorption and Synergistic Reduction of Nitrobenzene. *Chemosphere* **2012**, *87*, 655.

(17) Zhang, Y.; Li, Y.; Li, J.; Hu, L.; Zheng, X. Enhanced Removal of Nitrate by a Novel Composite: Nanoscale Zero Valent Iron Supported on Pillared Clay. *Chem. Eng. J.* **2011**, *171*, 526.

(18) Chen, W. F.; Parette, R.; Zou, J. Y.; Cannon, F. S.; Dempsey, B. A. Arsenic Removal by Iron-Modified Activated Carbon. *Water Res.* **2007**, *41*, 1851.

(19) Kanel, S. R.; Manning, B.; Charlet, L.; Choi, H. Removal of Arsenic(III) from Groundwater by Nanoscale Zero-Valent Iron. *Environ. Sci. Technol.* **2005**, *39*, 1291.

(20) Fu, F.; Han, W.; Huang, C.; Tang, B.; Hu, M. Removal of Cr(VI) from Wastewater by Supported Nanoscale Zero-Valent Iron on Granular Activated Carbon. *Desalin. Water Treat.* **2013**, *51*, 2680.

(21) Shi, L. N.; Zhang, X.; Chen, Z. L. Removal of Chromium (VI) from Wastewater Using Bentonite-Supported Nanoscale Zero-Valent Iron. *Water Res.* **2011**, *45*, 886.

(22) Lv, X. S.; Xu, J.; Jiang, G. M.; Xu, X. H. Removal of Chromium(VI) from Wastewater by Nanoscale Zero-Valent Iron Particles Supported on Multiwalled Carbon Nanotubes. *Chemosphere* **2011**, *85*, 1204.

(23) Wang, Q.; Snyder, S.; Kim, J.; Choi, H. Aqueous Ethanol Modified Nanoscale Zerovalent Iron in Bromate Reduction: Synthesis, Characterization, and Reactivity. *Environ. Sci. Technol.* **2009**, *43*, 3292.

(24) Phenrat, T.; Saleh, N.; Sirk, K.; Tilton, R. D.; Lowry, G. V. Aggregation and Sedimentation of Aqueous Nanoscale Zerovalent Iron Dispersions. *Environ. Sci. Technol.* **2006**, *41*, 284.

(25) Zhan, J.; Zheng, T.; Piringer, G.; Day, C.; McPherson, G. L.; Lu, Y.; Papadopoulos, K.; John, V. T. Transport Characteristics of Nanoscale Functional Zerovalent Iron/Silica Composites for in Situ Remediation of Trichloroethylene. *Environ. Sci. Technol.* **2008**, *42*, 8871.

(26) Li, Y.; Zhang, Y.; Li, J.; Zheng, X. Enhanced Removal of Pentachlorophenol by a Novel Composite: Nanoscale Zero Valent Iron Immobilized on Organobentonite. *Environ. Pollut.* **2011**, *159*, 3744.

(27) Jüntgen, H. Activated Carbon as Catalyst Support: A Review of New Research Results. *Fuel* **1986**, *65*, 1436.

(28) Tseng, H. H.; Su, J. G.; Liang, C. Synthesis of Granular Activated Carbon/Zero Valent Iron Composites for Simultaneous Adsorption/Dechlorination of Trichloroethylene. *J. Hazard. Mater.* **2011**, *192*, 500.

(29) Boehm, H. P. Some Aspects of the Surface Chemistry of Carbon Blacks and Other Carbons. *Carbon* **1994**, *32*, 759.

(30) Noh, J. S.; Schwarz, J. A. Effect of HNO_3 Treatment on the Surface Acidity of Activated Carbons. *Carbon* **1990**, *28*, 675.

(31) Dhaouadi, A.; Monser, L.; Adhoum, N. Removal of Rotenone Insecticide by Adsorption onto Chemically Modified Activated Carbons. *J. Hazard. Mater.* **2010**, *181*, 692.

(32) Wang, C.; Baer, D. R.; Amonette, J. E.; Engelhard, M. H.; Antony, J.; Qiang, Y. Morphology and Electronic Structure of the Oxide Shell on the Surface of Iron Nanoparticles. *J. Am. Chem. Soc.* **2009**, *131*, 8824.
(33) Nurmi, J. T.; Tratnyek, P. G.; Sarathy, V.; Baer, D. R.; Amonette, J. E.; Pecher, K.; Wang, C.; Linehan, J. C.; Matson, D. W.; Penn, R. L.; Driessen, M. D. Characterization and Properties of Metallic Iron Nanoparticles: Spectroscopy, Electrochemistry, and Kinetics. *Environ. Sci. Technol.* **2005**, *39*, 1221.
(34) Kubilay, Ş.; Gürkan, R.; Savran, A.; Şahan, T. Removal of Cu(II), Zn(II) and Co(II) Ions from Aqueous Solutions by Adsorption onto Natural Bentonite. *Adsorption* **2007**, *13*, 41.
(35) Deliyanni, E.; Bandosz, T. J. Importance of Carbon Surface Chemistry in Development of Iron−Carbon Composite Adsorbents for Arsenate Removal. *J. Hazard. Mater.* **2011**, *186*, 667.
(36) Rivera-Utrilla, J.; Sánchez-Polo, M.; Gómez-Serrano, V.; Álvarez, P. M.; Alvim-Ferraz, M. C. M.; Dias, J. M. Activated Carbon Modifications to Enhance Its Water Treatment Applications. An Overview. *J. Hazard. Mater.* **2011**, *187*, 1.
(37) Cheng, R.; Wang, J. L.; Zhang, W. X. Comparison of Reductive Dechlorination of p-Chlorophenol Using Fe^0 and Nanosized Fe^0. *J. Hazard. Mater.* **2007**, *144*, 334.
(38) Chen, Z. X.; Jin, X. Y.; Chen, Z.; Megharaj, M.; Naidu, R. Removal of Methyl Orange from Aqueous Solution Using Bentonite-Supported Nanoscale Zero-Valent Iron. *J. Colloid Interface Sci.* **2011**, *363*, 601.
(39) Parshetti, G. K.; Doong, R. A. Dechlorination of Chlorinated Hydrocarbons by Bimetallic Ni/Fe Immobilized on Polyethylene Glycol-Grafted Microfiltration Membranes under Anoxic Conditions. *Chemosphere* **2012**, *86*, 392.
(40) Shih, Y. H.; Hsu, C. Y.; Su, Y. F. Reduction of Hexachlorobenzene by Nanoscale Zero-Valent Iron: Kinetics, pH Effect, and Degradation Mechanism. *Sep. Purif. Technol.* **2011**, *76*, 268.
(41) Bao, M. L.; Griffini, O.; Santianni, D.; Barbieri, K.; Burrini, D.; Pantani, F. Removal of Bromate Ion from Water Using Granular Activated Carbon. *Water Res.* **1999**, *33*, 2959.
(42) Çelebi, O.; Üzüm, Ç.; Shahwan, T.; Erten, H. N. A Radiotracer Study of the Adsorption Behavior of Aqueous Ba^{2+} Ions on Nanoparticles of Zero-Valent Iron. *J. Hazard. Mater.* **2007**, *148*, 761.